ACS OMEGA

Open Access

http://pubs.acs.org/journal/acsodf

Article

Sensitive and Direct Analysis of *Pseudomonas aeruginosa* through Self-Primer-Assisted Chain Extension and CRISPR-Cas12a-Based Color Reaction

Jiangchun Hu,[‡] Ling Liang,[‡] Mingfang He,* and Yongping Lu*

Cite This: *ACS Omega* 2023, 8, 34852−34858

Read Online

ACCESS | Metrics & More | Article Recommendations | Supporting Information

ABSTRACT: *Pseudomonas aeruginosa* (*P. aeruginosa*) is a common opportunistic Gram-negative pathogen that may cause infections to immunocompromised patients. However, sensitive and reliable analysis of *P. aeruginosa* remains a huge challenge. In this method, target recognition assists the formation of a self-primer and initiates single-stranded chain production. The produced single-stranded DNA chain is identified by CRISPR-Cas12a, and consequently, the *trans*-cleavage activity of the Cas12a enzyme is activated to parallelly digest Ag^+ aptamer sequences that are chelated with silver ions (Ag^+). The released Ag^+ reacted with 3,3′,5,5′-tetramethylbenzidine (TMB) for coloring. Compared with the traditional color developing strategies, which mainly rely on the DNA hybridization, the color developing strategy in this approach exhibits a higher efficiency due to the robust *trans*-cleavage activity of the Cas12a enzyme. Consequently, the method shows a low limit of detection of a wide detection of 5 orders of magnitudes and a low limit of detection of 21 cfu/mL, holding a promising prospect in early diagnosis of infections. Herein, we develop a sensitive and reliable method for direct and colorimetric detection of *P. aeruginosa* by integrating self-primer-assisted chain production and CRISPR-Cas12a-based color reaction and believe that the established approach will facilitate the development of bacteria-analyzing sensors.

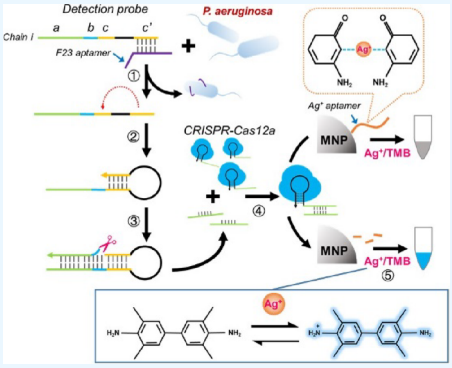

1. INTRODUCTION

Pseudomonas aeruginosa (*P. aeruginosa*), as an opportunistic Gram-negative pathogen, has attracted increasing attention in postoperative infection and posed an emerging threat to human health.[1−3] *P. aeruginosa* possesses widespread habitats, such as water, air, animals, and humans, making it hard to control.[4,5] The significant roles of *P. aeruginosa* in causing osteoarticular infections and causing long-term chronic diseases in immunocompromised patients promote the development of a reliable and sensitive method.[6]

The immunological approach, as one of the common methods for *P. aeruginosa* detection, is developed based on the high affinity and selectivity between the antibody and antigen.[7,8] The immunological approach has been widely used in quantitative or qualitative analysis of *P. aeruginosa*.[9,10] However, the immunological approach is criticized by the low sensitivity and tedious labor intensity, which greatly hinder its further applications.[11,12] The polymerase chain reaction (PCR) method is also widely utilized in identifying *P. aeruginosa* by analyzing target gene sequences.[13−15] Despite the fact that PCR exhibits high sensitivity and stability in quantifying *P. aeruginosa*, it possesses several shortcomings, including the requirement of thermal cycle, complicated primer design, and cumbersome equipment. An aptamer, as a kind of oligonucleotide sequence that is screened by systematic evolution of ligands by exponential enrichment (SELEX), is capable of specifically binding with a target molecule with high affinity.[16,17] The programmability and availability of the aptamer made it a promising transducer capable of converting protein signals to nucleic acid signals, and consequently, the aptamer is widely applied in established novel biosensors.[18,19] In recent years, a variety of aptasensors have been developed based on different signal transducers, such as fluorescence, colorimetry, and electrochemistry.[20−23] For example, Li *et al.* proposed a fluorescence assay for sensitive and label-free bacterial detection by using an established cascade signal amplification strategy.[24] Based on the Exo-III enzyme-assisted chain recycle and rolling circle amplification-based signal amplification, the method exhibited a wide detection range of 5 orders of magnitudes and a low limit of detection. Despite the fact that fluorescence assay showed a promising prospect in determination of *P. aeruginosa*, the essential requirement of equipment to read fluorescence signals limited its further applications in resource-limited conditions. Colori-

Received: June 13, 2023
Accepted: August 31, 2023
Published: September 11, 2023

metric assays made it possible to read results directly with the naked eye.[25−27] These methods usually use signal-stranded DNA (ssDNA) sequences to regulate the aggregation and dispersion of gold nanoparticles (AuNPs) and thus to induce color development. The hybridization between the ssDNA sequences was one-to-one signal transduction that limited high-efficient aggregation of AuNPs.[28]

Clustered regularly interspaced short palindromic repeats/CRISPR-associated (CRISPR/Cas), which is an RNA-guided component from the immune system of bacteria, has been extensively harnessed for developing novel biosensors.[29−33] For example, Shin *et al.* developed an enhanced CRISPR/Cas-based fluorescence assay for reliable and sensitive detection of bacteria.[34] In addition, Han *et al.* proposed an isothermal amplification strategy by employing Cas12a-based primer production for sensitive nucleic acid quantification.[35] The *trans*-cleavage activity of CRISPR-Cas12a enables highly efficient digestion of ssDNA sequences after recognizing target sequences,[36] making it a promising tool to develop a sensitive and reliable colorimetric method.[37,38]

Herein, we propose a novel colorimetric approach for sensitive and reliable *P. aeruginosa* analysis by integrating self-primer-based production of ssDNA and CRISPR-Cas12a-assisted color development. The two signal-amplifying processes, including the chain extension and *trans*-cleavage of Cas12a, endow the method with high sensitivity. In addition, the silver ions (Ag^+) were chelated by aptamer sequences via the interaction between Ag^+ and the N3 of cytosine (C), forming a strong and stable "C-Ag^+-C" hairpin structure.[28] The digestion of the aptamer by the Cas12a enzyme released Ag^+ to oxidize 3,3′,5,5′-tetramethylbenzidine (TMB) for coloring. The solution that contained oxidized TMB (TMBox) had a blue color.[39,40]

2. EXPERIMENTAL SECTION

2.1. Reagents and Apparatus. Nt.BstNBI, phi29 polymerase, Engen Lba Cas12a (Cpf1, 100 μM), and deoxynucleotide (dNTP) solution mix were provided by New England Biolabs (Beijing, China). SYBR Green I was obtained from Life Technologies (Carlsbad, CA). Silver nitrate ($AgNO_3$) and TMB (HPLC, ≥99%) were purchased from Shanghai Huzhen Biotechnology Co., Ltd. (Shanghai, China). COOH-MNPs (carboxyl-modified magnetic nanoparticles, 10 mg/mL, 1000 nm) were obtained from Xi'an Ruixi Biotechnology Co., Ltd. (Xi'an, China). All chemical reagents used in this research were of analytical grade. All the oligonucleotides (Table 1), such as the F23 aptamer and detection probe, were synthesized and purified by Sangon Biological Engineering and Technology & Services Co., Ltd. (Shanghai, China). *P. aeruginosa*, *Staphylococcus aureus* (*S. aureus*, ATCC 29213), and *Escherichia coli* (*E. coli*, ATCC 25922) were obtained from the American Type Culture Collection (ATCC).

Table 1. DNA and RNA Sequences Used in This Study

title	sequence (5′−3′)
Ag^+ aptamer	CCT CCC TCC CTC CCT TTT TCC CAC CCA CCC ACC
crRNA	UAA UUU CUA CUA AGU GUA GAU UU A AAG AAG AUG GUA UGU GG
chain i	AAA GAA GAT GGT ATG TGG AAT CCG ACT CTT TCG TCC TTT TTT AAG GAC GAA
F23 aptamer	CCC CCG TTG CTT TCG CTT TTC CTT TCG CTT TTG TTC GTT TCG TCC CTG CTT CCT TTC TTG

2.2. Assembly and Feasibility of the Detection Probe. The assembly of the detection probe was performed following the steps: 2 μL of F23 aptamer (10 μM) and 2 μL of ssDNA (10 μM) sequences were mixed in a tube containing 16 μL of PBS buffer. The mixture was then incubated at 90 °C for 10 min and cooled to room temperature. The fluorescence detection probe was assembled with the same procedures. To test the feasibility of the detection probe in detecting target bacteria, 10 μL of assembled detection probe was incubated with 2 μL of *P. aeruginosa*, and the mixture was incubated at room temperature for 20 min. The fluorescence signals before and after the addition of *P. aeruginosa* were recorded.

2.3. Detection Procedures of the Established Approach. Two microliters of *P. aeruginosa* solution, 2 μL of detection probe, and 16 μL of PBS buffer were mixed, and the mixture was incubated for 15 min. Afterward, 2 μL of phi29 enzyme (3 U/L), 2 μL of Nt.BstNBI (0.5 U/L), and 6 μL of NEB buffer were added in the mixture. The mixture was then heated to 70 °C for 5 min to inactivate the enzymes. Two microliters of Cas12a enzyme (50 nM), 2 μL of crRNA (2 μM), and 16 μL of Apt−MNPs were added to the mixture and reacted at room temperature for 15 min. Ten microliters of $AgNO_3$ was added to the mixture and reacted at room temperature for 10 min. After magnetic-based separation and washing by PBS buffer, 10 μL of TMB (5 mM) was added to the mixture, and the mixture was incubated at room temperature for 20 min in a dark environment.

3. RESULTS AND DISCUSSION

3.1. The Working Mechanism of the Established Approach. The working mechanism of the established approach is illustrated in Figure 1. In the method, a detection probe is designed to be composed of two sequences, one is the chain i sequence containing four functional sections and the other one is an F23 aptamer (a *P. aeruginosa*-specific aptamer) that can specifically bind the surface protein of *P. aeruginosa*. In detail, the *c*′ section is complementary with the *c* section, and the *b* section can transcribe a nicking site. In the detection probe, F23 aptamer sequences are partially complementary with the *c*′ section, blocking it from hybridizing with the *c* section. In the presence of *P. aeruginosa*, it can specifically bind with the aptamer sequence, exposing the *c*′ section. The exposed *c*′ section binds with the *c* section, forming a self-primer. Under the assistance of the phi29 enzyme, an ssDNA chain containing a nicking site is added to the 3′ terminal of the *c*′ section. The nicking site can be cut by an endonuclease, generating a gap and cooperating with the phi29 enzyme to produce large amounts of *a*′ sequences. The *a*′ sequences can be recognized by the CRISPR-Cas12a system and activate the *trans*-cleavage activity of the Cas12a enzyme to induce the color reaction.

In the CRISPR-Cas12a-based color reaction, Ag^+ is chelated by the Ag^+ aptamer sequences and the Ag^+-Ag^+ aptamer complex is pre-coupled to magnetic nanoparticles (Ag^+-Apt−MNPs). When *P. aeruginosa* exists in the sensing system, the *trans*-cleavage activity of Cas12a is activated to cut the aptamer in Ag^+-Apt−MNPs, releasing Ag^+. After magnetic isolation, the sediment comprising only MNPs is removed and the supernatant containing Ag^+ is exploited to oxidize TMB for color reaction. The solution that contained oxidized TMB (TMBox) had a blue color.[28,39,40] If *P. aeruginosa* is absent in the sensing

https://doi.org/10.1021/acsomega.3c04180
ACS Omega 2023, 8, 34852−34858

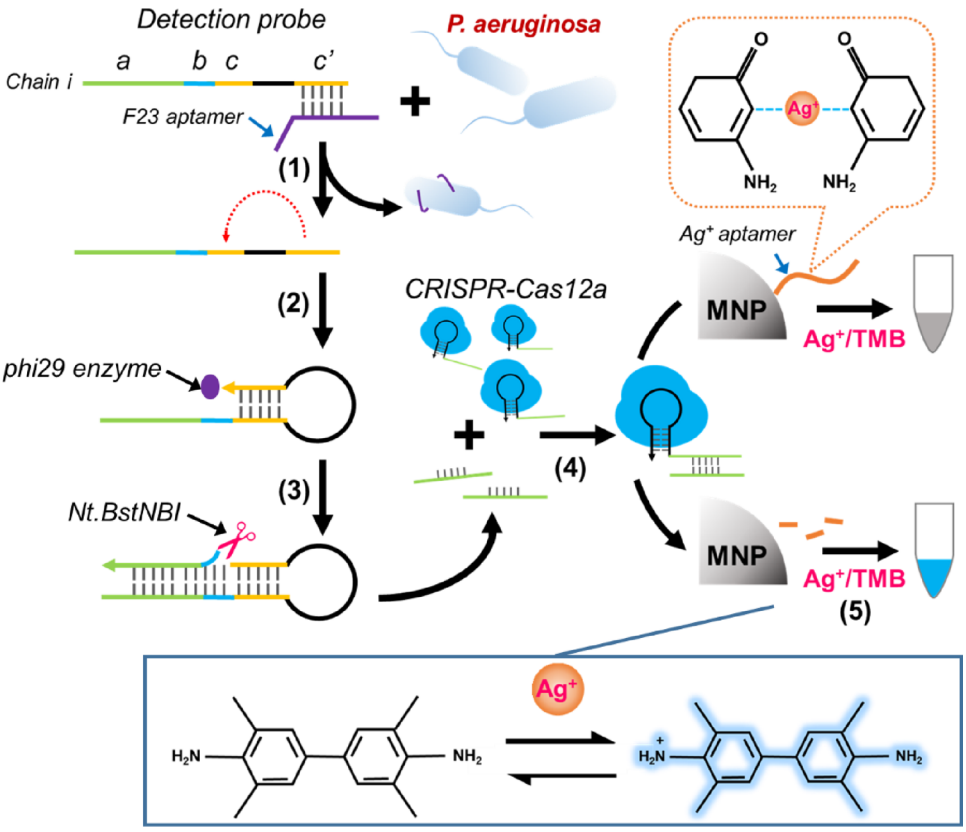

Figure 1. Schematic of the CRISPR-Cas12a-based colorimetric assay. (1) target recognition; (2) hybridization of *c* and *c*′; (3) single-stranded chain (Ag^+ aptamer sequences) production; (4) CRISPR-Cas12a-based cleavage of single-stranded chain (Ag^+ aptamer sequences); (5) mechanism of the color reaction.

system, Ag^+-Apt−MNPs is removed after magnetic separation, and TMB cannot be oxidized by the supernatant.

3.2. Feasibility of the Self-Primer-Assisted Chain Extension and *trans*-Cleavage Activity of the CRISPR-Cas12a System. Target recognition initiated the formation of a self-primer and determined the specificity of the established approach. Thus, we first investigated the target recognition capability of the established approach through a fluorescence assay (Figure 2A). In the fluorescence assay, the fluorescence moiety (FAM) and corresponding quenching moiety were labeled on the terminals of the *c* section and *c*′ section. The F23 aptamer partially bound with the *c*′ section, blocking the formation of a self-primer. The existence of *P. aeruginosa* initiated the formation of a self-primer, causing the quenching of the FAM signal. As shown in Figure 2B, the FAM signal was significantly higher when *P. aeruginosa* was absent in the sensing system than when *P. aeruginosa* existed, indicating successful formation of a self-primer after target recognition. Meanwhile, no significant change of FAM signals was observed when the detection probes were incubated with *S. aureus* and *E. coli*, indicating a high selectivity of the detection probe. SYBR Green I is a dye that binds to the double helix groove region of dsDNA. In the free state, SYBR Green I fluoresces weakly, but once bound to double-stranded DNA, the fluorescence is greatly enhanced. Therefore, SYBR Green I was exploited to characterize the chain extension process. The result in Figure 2C showed a gradually increased fluorescence signal when *P. aeruginosa* and phi29 enzyme existed in the sensing system. On the contrary, the SYBR signal showed no enhancements compared with the control group when *P. aeruginosa* or phi29 enzyme was absent in the system. The result in the presence or absence of Nt.BstNBI is shown in Figure. S1. We recorded the SYBR Green I signals in in the presence or absence of Nt.BstNBI at 30 min and obtained no significant difference between the two groups due to the fact that the chain production process was terminated. To test the *trans*-cleavage activity of CRISPR-Cas12a, an ssDNA probe that is labeled with FAM and BHQ on the two terminals was added to the sensing system. In the existence of *P. aeruginosa*, a greatly elevated FAM signal was observed, indicating that the ssDNA probe was cut by the active Cas12a enzyme (Figure 2D). A fluorescence assay was used to characterize the assembly of Apt−MNPs. In this assay, the terminal of aptamer sequences was labeled with the FAM moiety. After the assembly of Apt−MNPs, the fluorescence signals were recorded. The result in Figure. S2 showed significantly higher fluorescence signals of the Apt−MNPs complex compared to aptamer sequences alone, indicating the successful assembly of Apt−MNPs.

3.3. Optimization of Experimental Parameters. For a better detection performance, we optimized the experimental parameters, including the concentrations of phi29 enzyme and endonuclease and incubation time for CRISPR-Cas12a-based color reaction. The approach was applied to detect 5×10^5 cfu/mL *P. aeruginosa*, and the parameters were optimized. To quantitatively compare the detection performance, the characteristic UV−vis absorption peak at 652 nm was recorded. The result in Figure 3A showed a gradually increased absorbance when the concentration of the phi29 enzyme ranged from 1 to 3 U/L, and no more increments could be observed when the sensing system was incubated with more phi29 enzyme. Thus, 3 U/L phi29 enzyme was selected in the following experiments.

https://doi.org/10.1021/acsomega.3c04180
ACS Omega 2023, 8, 34852−34858

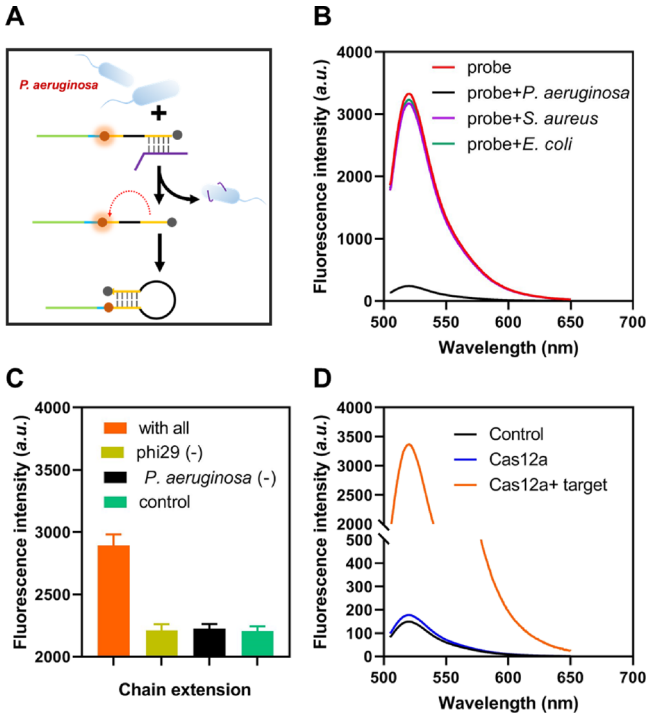

Figure 2. Construction of the detection probe and feasibility of *trans*-cleavage activity of the CRISPR-Cas12a system. (A) Schematic mechanism of the fluorescence assay. (B) Fluorescence spectrum of the detection probe when *P. aeruginosa* existed or not. (C) SYBR Green I fluorescence during the chain extension process when *P. aeruginosa* and phi29 enzyme existed in the sensing system or not. Data were expressed as the mean ± standard deviations; $n = 3$ technical replicates. (D) Fluorescence spectrum of the sensing system when the Cas12a enzyme was activated or not.

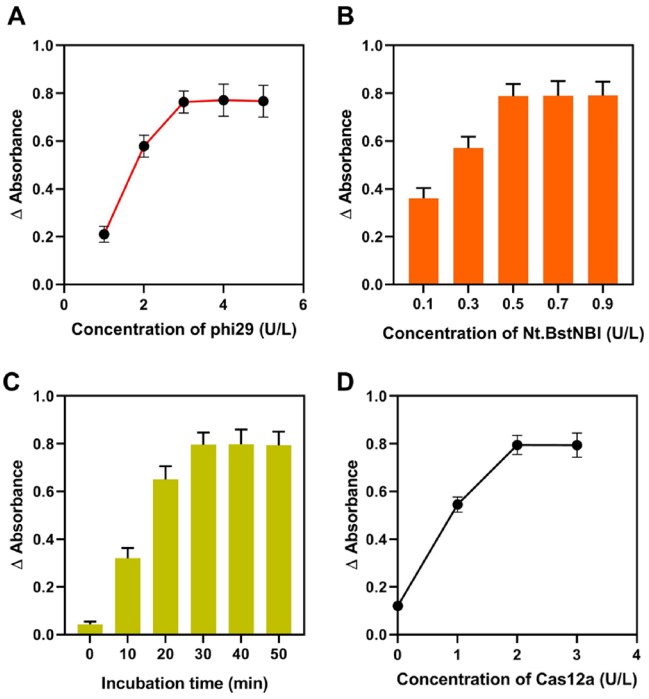

Figure 3. Optimization of experimental conditions. Δ Absorbance (absorbance when the target existed minus absorbance of the blank group) of the approach with different concentrations of phi29 enzyme (A) and Nt.BstNBI (B), different incubation times (C), and Cas12a concentration (D). Data were expressed as the mean ± standard deviations; $n = 3$ technical replicates. The concentration of *P. aeruginosa* was 5×10^5 cfu/mL.

With constant 3 U/L phi29 enzyme, we then optimized the concentration of endonuclease. From the result in Figure 3B, the absorbance of the approach elevated when the concentration of endonuclease ranged from 0.1 to 0.5 U/L. When the system was added with more endonuclease, no significant increments could be recorded. Therefore, 0.5 U/L endonuclease was used in the following experiments. Meanwhile, the incubation time for CRISPR-Cas12a-based color reaction was 30 min (Figure 3C). The concentration of the Cas12a enzyme is crucial for the cleavage of Ag^+ aptamer sequences, thus affecting the color reaction. The result in Figure 3D showed a gradually increased absorbance when the concentration of the Cas12a enzyme ranged from 0 to 2 U/L and reached an equilibrium with more Cas12a concentrations. The result in Figure. S3 demonstrated that the optimized number of bases selected for F23 aptamer binding with chain i was 10.

3.4. Analytical Performance of the Established Approach. Under the optimized experimental conditions, the detection performance of the established approach is evaluated. To test the sensitivity of the approach, different concentrations of *P. aeruginosa* samples were prepared. The established approach was then applied to quantify *P. aeruginosa*. Figure. S4 shows the color changes of the method when target bacteria existed or not, and the result in Figure 4A showed that the absorbance gradually elevated with the concentration of *P. aeruginosa* ranged from 10^2 to 10^6 cfu/mL. The recorded absorbance of the approach was correlated with the concentrations of the target.[41,42] The correlation equation between the absorbance and logarithmic concentrations of *P. aeruginosa* was $Y = 0.1448 \times \lg C + 0.008$, with the correlation coefficient of 0.9965 (Figure 4B). The limit of detection of the colorimetric approach was determined to be 21 cfu/mL, which is superior or comparable to former strategies for *P. aeruginosa* detection.[19,27,43] To investigate the selectivity of the established colorimetric approach, the method was employed to detect *P. aeruginosa* and other pathogens, including *E. coli* and *S. aureus*. The concentration of each bacterium is 10^5 cfu/mL. The result in Figure 4C showed a significantly enhanced absorbance in comparison with the negative controls when detecting *P. aeruginosa*. The absorbance of the approach exhibited neglectable enhancements when detecting other bacteria, suggesting a high specificity of the approach.

3.5. Real Sample Analysis. To verify the potential feasibility of the established colorimetric approach in real sample analysis, artificial samples were prepared by diluting *P. aeruginosa* using commercial serum. The method and traditional colony counting method were used to quantify *P. aeruginosa*. The result in Figure 5 showed that the calculated amount of *P. aeruginosa* by the established approach was positively correlated with the detected result by the colony counting method with a high correlation coefficient of 0.9897, indicating that the established approach could be potentially an alternative method for *P. aeruginosa* determination.

4. CONCLUSIONS

P. aeruginosa is a common pathogenic bacterium in nosocomial infection and causes osteoarticular infections in immunocompromised patients. Early determination of *P. aeruginosa* infection assists the management of disease. Herein, a sensitive and reliable approach has been constructed for direct and efficient

https://doi.org/10.1021/acsomega.3c04180
ACS Omega 2023, 8, 34852−34858

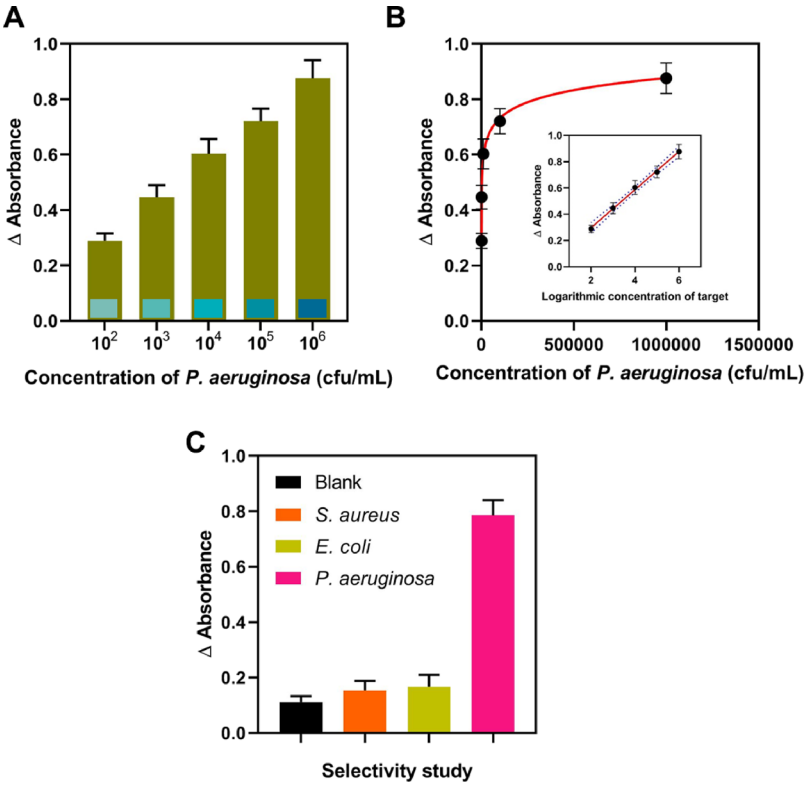

Figure 4. Analytical performance of the established approach. (A) Δ Absorbance (absorbance when the target existed minus absorbance of the blank group) of the approach when detecting different concentrations of *P. aeruginosa*. Inserted in the columns were the standardized color results. (B) Correlation between the Δ absorbance and the concentrations of *P. aeruginosa*. (C) Δ Absorbance of the approach when detecting different bacteria. Data were expressed as the mean ± standard deviations; n = 3 technical replicates.

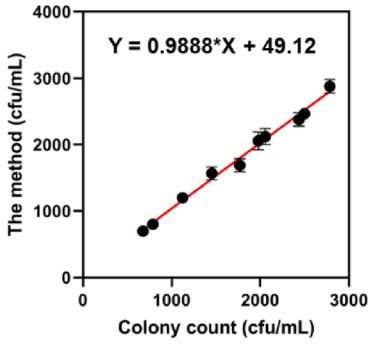

Figure 5. Correlation between the calculated amounts of *P. aeruginosa* by the method and colony counting method. *Y*: *P. aeruginosa* amount calculated by the method; *X*: *P. aeruginosa* amount obtained by the colony counting method. Data were expressed as the mean ± standard deviations; n = 3 technical replicates.

detection of *P. aeruginosa* by integrating self-primer-assisted chain extension and CRISPR-Cas12a-assisted color reaction. Compared with the traditional color developing strategies, which mainly rely on the DNA hybridization,[19−21] the color developing strategy in this approach exhibits a higher efficiency due to the robust *trans*-cleavage activity of the Cas12a enzyme. With the chain extension and *trans*-cleavage activity of Cas12a enzyme-based signal amplification, the method exhibited a wide detection of 5 orders of magnitudes and a low limit of detection of 21 cfu/mL. We believe that the proposed approach could be extended to diagnose disease biomarkers and assist the management of infections. Considering that the magnetic separation step is essential in the proposed system, which can interfere with the widespread practical application, we will focus on improving the stability and repeatability of the sensing system in the future by following standardized working practices or using novel separation procedures.

■ ASSOCIATED CONTENT

Supporting Information

The Supporting Information is available free of charge at https://pubs.acs.org/doi/10.1021/acsomega.3c04180.

SYBR Green I signals of the chain extension process when Nt.BstNBI existed or not (Figure. S1); FAM signals of aptamer sequences before and after assembly with MNPs (Figure. S2); A/A_0 result of the approach with different complementary numbers between the F23 aptamer and chain i (Figure. S3); color change and corresponding absorbance spectra of the TMBs when target bacteria existed (+) or not (−) (Figure. S4) (PDF)

■ AUTHOR INFORMATION

Corresponding Authors

Mingfang He − *Science and Technology Innovation Center, Guangyuan Central Hospital, Guangyuan City 628000 Sichuan Province, China*; Email: 3353068261@qq.com

Yongping Lu − *Science and Technology Innovation Center, Guangyuan Central Hospital, Guangyuan City 628000 Sichuan Province, China*; orcid.org/0000-0002-7958-551X; Email: luyongping_lyp@163.com

https://doi.org/10.1021/acsomega.3c04180
ACS Omega 2023, 8, 34852−34858

Authors

Jiangchun Hu − *Science and Technology Innovation Center, Guangyuan Central Hospital, Guangyuan City 628000 Sichuan Province, China*

Ling Liang − *Science and Technology Innovation Center, Guangyuan Central Hospital, Guangyuan City 628000 Sichuan Province, China*

Complete contact information is available at: https://pubs.acs.org/10.1021/acsomega.3c04180

Author Contributions

‡J.H. and L.L. were the co-first authors and contributed equally to this research. Y.L. and M.H.: conceptualization, methodology, validation, formal analysis, investigation, data curation, writing of the original draft, review and editing, visualization, project administration, and supervision. J.H. and L.L.: conceptualization, methodology, resources, and review and editing.

Notes

The authors declare no competing financial interest.

■ ACKNOWLEDGMENTS

This work was supported by the Guangyuan Central Hospital.

■ REFERENCES

(1) Marei, E. M. Isolation and Characterization of Pseudomonas aeruginosa and its Virulent Bacteriophages. *Pak. J. Biol. Sci.* **2020**, *23*, 491−500.

(2) Mielko, K. A.; Jablonski, S. J.; Milczewska, J.; Sands, D.; Lukaszewicz, M.; Mlynarz, P. Metabolomic studies of Pseudomonas aeruginosa. *World J. Microbiol. Biotechnol.* **2019**, *35*, 178.

(3) Sharma, G.; Rao, S.; Bansal, A.; Dang, S.; Gupta, S.; Gabrani, R. Pseudomonas aeruginosa biofilm: potential therapeutic targets. *Biologicals* **2014**, *42*, 1−7.

(4) Miyoshi-Akiyama, T.; Tada, T.; Ohmagari, N.; Viet Hung, N.; Tharavichitkul, P.; Pokhrel, B. M.; Gniadkowski, M.; Shimojima, M.; Kirikae, T. Emergence and Spread of Epidemic Multidrug-Resistant Pseudomonas aeruginosa. *Genome. Biol. Evol.* **2017**, *9*, 3238−3245.

(5) Ribera, A.; Benavent, E.; Lora-Tamayo, J.; Tubau, F.; Pedrero, S.; Cabo, X.; Ariza, J.; Murillo, O. Osteoarticular infection caused by MDR Pseudomonas aeruginosa: the benefits of combination therapy with colistin plus β-lactams. *J. Antimicrob. Chemother.* **2015**, *70*, 3357−3365.

(6) Seghrouchni, K.; van Delden, C.; Dominguez, D.; Benkabouche, M.; Bernard, L.; Assal, M.; Hoffmeyer, P.; Uckay, I. Remission after treatment of osteoarticular infections due to Pseudomonas aeruginosa versus *Staphylococcus aureus*: a case-controlled study. *Int. Orthop.* **2012**, *36*, 1065−1071.

(7) Khatami, S. H.; Karami, S.; Siahkouhi, H. R.; Taheri-Anganeh, M.; Fathi, J.; Aghazadeh Ghadim, M. B.; Taghvimi, S.; Shabaninejad, Z.; Tondro, G.; Karami, N.; Dolatshah, L.; Soltani Fard, E.; Movahedpour, A.; Darvishi, M. H. Aptamer-based biosensors for Pseudomonas aeruginosa detection. *Mol. Cell. Probes* **2022**, *66*, No. 101865.

(8) Zheng, X.; Gao, S.; Wu, J.; Hu, X. Recent Advances in Aptamer-Based Biosensors for Detection of Pseudomonas aeruginosa. *Front. Microbiol.* **2020**, *11*, No. 605229.

(9) Locke, A.; Fitzgerald, S.; Mahadevan-Jansen, A. Advances in Optical Detection of Human-Associated Pathogenic Bacteria. *Molecules* **2020**, *25*, 5256.

(10) Rajapaksha, P.; Elbourne, A.; Gangadoo, S.; Brown, R.; Cozzolino, D.; Chapman, J. A review of methods for the detection of pathogenic microorganisms. *Analyst* **2019**, *144*, 396−411.

(11) Yu, Z.; Qiu, C.; Huang, L.; Gao, Y.; Tang, D. Micro-electromechanical Microsystems-Supported Photothermal Immunoassay for Point-of-Care Testing of Aflatoxin B1 in Foodstuff. *Anal. Chem.* **2023**, *95*, 4212−4219.

(12) Zeng, R.; Qiu, M.; Wan, Q.; Huang, Z.; Liu, X.; Tang, D.; Knopp, D. Smartphone-Based Electrochemical Immunoassay for Point-of-Care Detection of SARS-CoV-2 Nucleocapsid Protein. *Anal. Chem.* **2022**, *94*, 15155−15161.

(13) Li, Y.; Hu, Y.; Chen, T.; Chen, Y.; Li, Y.; Zhou, H.; Yang, D. Advanced detection and sensing strategies of Pseudomonas aeruginosa and quorum sensing biomarkers: A review. *Talanta* **2022**, *240*, No. 123210.

(14) Li, H.; Bai, R.; Zhao, Z.; Tao, L.; Ma, M.; Ji, Z.; Jian, M.; Ding, Z.; Dai, X.; Bao, F.; Liu, A. Application of droplet digital PCR to detect the pathogens of infectious diseases. *Biosci. Rep.* **2018**, *38*, BSR20181170.

(15) Golpayegani, A.; Nodehi, R. N.; Rezaei, F.; Alimohammadi, M.; Douraghi, M. Real-time polymerase chain reaction assays for rapid detection and virulence evaluation of the environmental Pseudomonas aeruginosa isolates. *Mol. Biol. Rep.* **2019**, *46*, 4049−4061.

(16) Schmitz, F. R. W.; Cesca, K.; Valério, A.; de Oliveira, D.; Hotza, D. Colorimetric detection of Pseudomonas aeruginosa by aptamer-functionalized gold nanoparticles. *Appl. Microbiol. Biotechnol.* **2023**, *107*, 71−80.

(17) Zhang, X.; Xie, G.; Gou, D.; Luo, P.; Yao, Y.; Chen, H. A novel enzyme-free electrochemical biosensor for rapid detection of Pseudomonas aeruginosa based on high catalytic Cu-ZrMOF and conductive Super P. *Biosens. Bioelectron.* **2019**, *142*, No. 111486.

(18) Wang, H.; Chi, Z.; Cong, Y.; Wang, Z.; Jiang, F.; Geng, J.; Zhang, P.; Ju, P.; Dong, Q.; Liu, C. Development of a fluorescence assay for highly sensitive detection of Pseudomonas aeruginosa based on an aptamer-carbon dots/graphene oxide system. *RSC Adv.* **2018**, *8*, 32454−32460.

(19) Zhong, Z.; Gao, X.; Gao, R.; Jia, L. Selective capture and sensitive fluorometric determination of Pseudomonas aeruginosa by using aptamer modified magnetic nanoparticles. *Microchim. Acta* **2018**, *185*, 377.

(20) Lv, S.; Zhang, K.; Zeng, Y.; Tang, D. Double Photosystems-Based 'Z-Scheme' Photoelectrochemical Sensing Mode for Ultrasensitive Detection of Disease Biomarker Accompanying Three-Dimensional DNA Walker. *Anal. Chem.* **2018**, *90*, 7086−7093.

(21) Qiu, Z.; Shu, J.; Liu, J.; Tang, D. Dual-Channel Photoelectrochemical Ratiometric Aptasensor with up-Converting Nanocrystals Using Spatial-Resolved Technique on Homemade 3D Printed Device. *Anal. Chem.* **2019**, *91*, 1260−1268.

(22) Qiu, Z.; Shu, J.; Tang, D. Bioresponsive Release System for Visual Fluorescence Detection of Carcinoembryonic Antigen from Mesoporous Silica Nanocontainers Mediated Optical Color on Quantum Dot-Enzyme-Impregnated Paper. *Anal. Chem.* **2017**, *89*, 5152−5160.

(23) Gao, Z.; Qiu, Z.; Lu, M.; Shu, J.; Tang, D. Hybridization chain reaction-based colorimetric aptasensor of adenosine 5′-triphosphate on unmodified gold nanoparticles and two label-free hairpin probes. *Biosens. Bioelectron.* **2017**, *89*, 1006−1012.

(24) Li, Y.; Xu, F.; Zhang, J.; Huang, J.; Shen, D.; Ma, Y.; Wang, X.; Bian, Y.; Chen, Q. Sensitive and Label-free Detection of Bacteria in Osteomyelitis through Exo III-Assisted Cascade Signal Amplification. *ACS Omega* **2021**, *6*, 12223−12228.

(25) Wu, Z.; He, D.; Cui, B.; Jin, Z. A bimodal (SERS and colorimetric) aptasensor for the detection of Pseudomonas aeruginosa. *Microchim. Acta* **2018**, *185*, 528.

(26) Alhogail, S.; Suaifan, G. A. R. Y.; Bikker, F. J.; Kaman, W. E.; Weber, K.; Cialla-May, D.; Popp, J.; Zourob, M. M. Rapid Colorimetric Detection of Pseudomonas aeruginosa in Clinical Isolates Using a Magnetic Nanoparticle Biosensor. *ACS Omega* **2019**, *4*, 21684−21688.

(27) Das, R.; Dhiman, A.; Kapil, A.; Bansal, V.; Sharma, T. K. Aptamer-mediated colorimetric and electrochemical detection of Pseudomonas aeruginosa utilizing peroxidase-mimic activity of gold NanoZyme. *Anal. Bioanal. Chem.* **2019**, *411*, 1229−1238.

(28) Wei, L.; Wang, Z.; Wang, J.; Wang, X.; Chen, Y. Aptamer-based colorimetric detection of methicillin-resistant Staphylococcus aureus by using a CRISPR/Cas 12a system and recombinase polymerase amplification. *Anal. Chim. Acta* **2022**, *1230*, No. 340357.

(29) Han, J.; Shin, J.; Lee, E. S.; Cha, B. S.; Kim, S.; Jang, Y.; Kim, S.; Park, K. S. Cas 12a/blocker DNA-based multiplex nucleic acid detection system for diagnosis of high-risk human papillomavirus infection. *Biosens. Bioelectron.* **2023**, *232*, No. 115323.

(30) Li, Y.; Zeng, R.; Wang, W.; Xu, J.; Gong, H.; Li, L.; Li, M.; Tang, D. Size-Controlled Engineering Photoelectrochemical Biosensor for Human Papillomavirus-16 Based on CRISPR-Cas 12a-Induced Disassembly of Z-Scheme Heterojunctions. *ACS Sens.* **2022**, *7*, 1593−1601.
(31) Zeng, R.; Gong, H.; Li, Y.; Li, Y.; Lin, W.; Tang, D.; Knopp, D. CRISPR-Cas 12a-Derived Photoelectrochemical Biosensor for Point-Of-Care Diagnosis of Nucleic Acid. *Anal. Chem.* **2022**, *94*, 7442−7448.
(32) Wang, D. X.; Wang, J.; Du, Y. C.; Ma, J. Y.; Wang, S. Y.; Tang, A. N.; Kong, D. M. CRISPR/Cas 12a-based dual amplified biosensing system for sensitive and rapid detection of polynucleotide kinase/phosphatase. *Biosens. Bioelectron.* **2020**, *168*, No. 112556.
(33) Wang, D. X.; Wang, Y. X.; Wang, J.; Ma, J. Y.; Liu, B.; Tang, A. N.; Kong, D. M. MnO_2 nanosheets as a carrier and accelerator for improved live-cell biosensing application of CRISPR/Cas 12a. *Chem. Sci.* **2022**, *13*, 4364−4371.
(34) Shin, J.; Yoon, T.; Park, J.; Park, K. S. Sensitive and simultaneous detection of hygiene indicator bacteria using an enhanced CRISPR/Cas system in combination with a portable fluorescence detector. *Sens. Actuators, B* **2022**, *365*, No. 131871.
(35) Han, J.; Kim, S.; Kim, S.; Lee, E. S.; Cha, B. S.; Park, J. S.; Shin, J.; Jang, Y.; Park, K. S. Cas12a-based primer production enables isothermal amplification for nucleic acid detection. *Sens. Actuators, B* **2023**, *381*, No. 133401.
(36) Lee, S.; Nam, D.; Park, J. S.; Kim, S.; Lee, E. S.; Cha, B. S.; Park, K. S. Highly Efficient DNA Reporter for CRISPR/Cas12a-Based Specific and Sensitive Biosensor. *BioChip J.* **2022**, *16*, 463−470.
(37) Zhang, W. S.; Pan, J.; Li, F.; Zhu, M.; Xu, M.; Zhu, H.; Yu, Y.; Su, G. Reverse Transcription Recombinase Polymerase Amplification Coupled with CRISPR-Cas12a for Facile and Highly Sensitive Colorimetric SARS-CoV-2 Detection. *Anal. Chem.* **2021**, *93*, 4126−4133.
(38) Gong, S.; Wang, X.; Zhou, P.; Pan, W.; Li, N.; Tang, B. AND Logic-Gate-Based CRISPR/Cas12a Biosensing Platform for the Sensitive Colorimetric Detection of Dual miRNAs. *Anal. Chem.* **2022**, *94*, 15839−15846.
(39) Yan, Z.; Yuan, H.; Zhao, Q.; Xing, L.; Zheng, X.; Wang, W.; Zhao, Y.; Yu, Y.; Hu, L.; Yao, W. Recent developments of nanoenzyme-based colorimetric sensors for heavy metal detection and the interaction mechanism. *Analyst* **2020**, *145*, 3173−3187.
(40) Amalraj, A.; Narayanan, M.; Perumal, P. Highly efficient peroxidase-like activity of a metal-oxide-incorporated CeO(2)-MIL-(Fe) metal-organic framework and its application in the colorimetric detection of melamine and mercury ions via induced hydrogen and covalent bonds. *Analyst* **2022**, *147*, 3234−3247.
(41) Ren, R.; Cai, G.; Yu, Z.; Zeng, Y.; Tang, D. Metal-Polydopamine Framework: An Innovative Signal-Generation Tag for Colorimetric Immunoassay. *Anal. Chem.* **2018**, *90*, 11099−11105.
(42) Yu, Z.; Gong, H.; Li, M.; Tang, D. Hollow prussian blue nanozyme-richened liposome for artificial neural network-assisted multimodal colorimetric-photothermal immunoassay on smartphone. *Biosens. Bioelectron.* **2022**, *218*, No. 114751.
(43) Gao, R.; Zhong, Z.; Gao, X.; Jia, L. Graphene Oxide Quantum Dots Assisted Construction of Fluorescent Aptasensor for Rapid Detection of Pseudomonas aeruginosa in Food Samples. *J. Agric. Food Chem.* **2018**, *66*, 10898−10905.

https://doi.org/10.1021/acsomega.3c04180
ACS Omega 2023, 8, 34852−34858